[CANCER RESEARCH 63, 4698–4704, August 1, 2003]

Suppression of Prostate Tumor Growth by U19, a Novel Testosterone-regulated Apoptosis Inducer[1]

Wuhan Xiao, Qiuheng Zhang, Feng Jiang, Michael Pins, James M. Kozlowski, and Zhou Wang[2]

Departments of Urology [W. X., Q. Z., F. J., J. M. K., Z. W.], Molecular Pharmacology and Biological Chemistry [Z. W.], and Pathology [M. P.], The Robert H. Lurie Comprehensive Cancer Center [M. P., J. M. K., Z. W.], Northwestern University Medical School, Chicago, Illinois 60611

ABSTRACT

Androgens control prostate homeostasis and regulate androgen response genes. Here, we report the identification and characterization of *U19*, a novel testosterone-regulated apoptosis inducer with tumor suppressive activity. *U19* is an evolutionarily conserved protein expressed in many human tissues, with the most abundant expression in the prostate, bone marrow, kidney, and lymph nodes. Overexpression of *U19* in 12 surveyed cell lines induced apoptosis, and new protein synthesis is required for apoptosis induction. Expression of *U19* in xenograft prostate tumors markedly induced apoptosis and inhibited tumor growth *in vivo*. Consistent with its tumor-suppressive role, *U19* down-regulation was observed in all of the surveyed prostate cancer cell lines and in 19 of 23 clinical human prostate tumor specimens. Loss of heterozygosity analysis revealed *U19* allelic loss in 19 of the 23 specimens. Furthermore, two of the specimens had homozygous *U19* deletions, and one specimen had hypermethylated *U19* promoter, indicating that *U19* can be inactivated genetically or epigenetically. These observations suggest that *U19* is growth inhibitory and tumor suppressive and that the disruption of androgen-dependent growth inhibition via *U19* down-regulation is commonly associated with prostate cancer progression.

INTRODUCTION

Androgens play an important role in prostate cancer progression. It is generally thought that higher than usual levels of androgens is a risk factor for prostate cancer because androgens are required for prostate growth (1). Humans with androgen deficiency, such as eunuchs or individuals with inactive 5α-reductase, have underdeveloped prostate, and no prostate cancer case has been reported among these individuals (1). Androgen administration has been demonstrated to induce or accelerate prostate cancer in some animal models (2, 3). Furthermore, prostate cancers are, in general, androgen dependent initially and respond to androgen ablation therapy. The above-mentioned observations suggest that androgens are growth stimulatory in the prostate and that excessive androgen action is likely to be a causative factor in prostate carcinogenesis. However, this concept does not correlate with some observations. For example, as individuals age, the risk of prostate cancer increases dramatically, whereas androgen levels fall (4–6). The unusually high androgen levels may not exist in aging males and are thus unlikely to be a causative factor of prostate cancer.

Despite the different opinions discussed above, the importance of androgens in prostate cancer progression is well recognized. The elucidation of the androgen action pathway, a cascade of molecular and cellular events triggered by androgen manipulation leading to cell proliferation, apoptosis, and/or differentiation, would provide insights into the roles of androgens in prostate cancer progression.

The effects of androgens on the prostate are complex. The prostate will undergo extensive apoptosis and regression if androgens are ablated (7). Androgens stimulate proliferation in a regressed prostate, but not in a fully grown prostate. It was postulated by Bruchovsky *et al.* (8) that androgens induce not only mitogenic factors but also nullifiers that negate proliferation once the number of cells reaches the normal level. The homeostasis of the prostate should require balanced activities of the androgen-dependent mitogenic factors and nullifiers. Excessive activation of mitogenic factors and/or inactivation of nullifiers could conceivably lead to uncontrolled growth and, eventually, cancer. Because androgen action is mediated through androgen receptor, a ligand-dependent transcription factor (9), the mitogenic factors and nullifiers are likely to be encoded by androgen response genes. We have identified more than 20 androgen response genes in the rat ventral prostate using a gene expression screen (10). This report describes the characterization of one of the identified genes, *U19* (10), as a novel testosterone-regulated apoptosis inducer with tumor-suppressive activity. Our studies provide new insights into the mechanisms of androgen action and the roles of androgens in prostate cancer progression.

MATERIALS AND METHODS

Cell Lines and Tissue Samples. The LNCaP, PC3, DU145, and TSU cell lines were obtained from American Type Culture Collection. Dunning tumor cell lines G, AT1, AT2, AT3.1, AT6.1, and MatLyLu were provided by Allen Gao (University of Pittsburgh). The NIH3T3 cell line was provided by Ali Shah, and HeLa cells were provided by David Klumpp (Northwestern University). Human multiple tissue polyadenylated RNA Northern blot membranes were purchased from Clontech (catalogue numbers 7780-1 and 7784-1; Palo Alto, CA).

All archival patient specimens (Gleason score, 7–10) were from Department of Pathology, Northwestern Memorial Hospital. The specimens were cut into 5–7-μm sections and then stained with H&E on membrane-coated glass slides (catalogue number 11505134; Nuhsbaum, McHenry, IL). About 5,000–10,000 cells from benign prostate tissue and distinct neoplastic foci were captured separately in the same stained sections using LCM[3] (Leica LMD system; Nuhsbaum). Genomic DNA was isolated and dissolved in a 50-μl final volume using the High Pure PCR Template Preparation Kit (Roche, Indianapolis, IN).

5′- and 3′-RACE and Low Stringency Hybridization. The 3′ region of mouse *U19* cDNA was screened from a mouse cDNA library using low stringency hybridization with rat *U19* cDNA as a probe. The 5′-RACE was performed for cloning the 5′ region of mouse *U19* cDNA using primers 5′-GTTCAACTCCACCAGTCACAG-3′,5′-CGGTGACAAGTAGCATCAGC-3′,5′-CTGAAGTCCTGTACTGTGGC-3′, and 5′-CACAACTACTCATCTG-GTCC-3′. Similarly, the 5′-RACE and 3′-RACE were performed for cloning the full-length of human *U19* cDNA using primers 5′-TGATACTGGAGGAT-GTCGGC-3′,5′-CACAACTACTCATCTGGTCC-3′,5′-GCTGGGGACATCTT-ATCTTC-3′,5′-CAGTGATTGTTGCTGCTGAG-3′, and 5′-CTCAGCAGCAA-CATCACTGT-3′.

Vector Construction. The cDNAs of rat and human *U19* were cloned into pEGFP C1, pEGFP N3, PM, and pIRES2-EGFP (Clontech) by PCR. Deletion mutagenesis of *U19* was generated by PCR and cloned into above first three

Received 1/14/03; accepted 5/28/03.

The costs of publication of this article were defrayed in part by the payment of page charges. This article must therefore be hereby marked *advertisement* in accordance with 18 U.S.C. Section 1734 solely to indicate this fact.

[1] Supported in part by NIH Grant R01 DK51193 and NIH P50 CA90386 Prostate Cancer Specialized Programs of Research Excellence.

[2] To whom requests for reprints should be addressed, at Northwestern University Medical School, Department of Urology, Tary 11-715, Chicago, IL 60611. E-mail: wangz@northwestern.edu.

[3] The abbreviations used are: LCM, laser capture microdissection; aa, amino acid(s); RACE, rapid amplification of cDNA ends; GFP, green fluorescent protein; 4-OHT, 4-hydroxytamoxifen; TUNEL, terminal deoxynucleotidyl transferase-mediated nick end labeling; LOH, loss of heterozygosity; ER, estrogen receptor; Z-VAD, Z-Val-Ala-DL-Asp-fluoromethylketon; ELL, eleven nineteen lysine-rich leukemia gene; TMR, tetramethyl rhodamine.

vectors. The plasmids containing ER domain were kindly provided by G. Evan (University of California San Francisco, San Francisco, CA). The ER ligand-binding domain was cut with *Bam*HI/*Eco*RI and recloned into pEGFP-*U19* to generate a tripartite fusion protein. All constructs were verified by sequencing and transfected using LipofectAMINE (Invitrogen) for LNCaP, DU145, TSU, and Dunning tumor cell lines; SuperFect reagent (Qiagen, Valencia, CA) for NIH3T3 and HeLa; or FuGENE 6 (Roche) for PC3. G418 (500 μg/ml) was used for stable selection of positive clones.

Cell Death Assays. In flow cytometry analysis, cells cultured under the indicated conditions were harvested for staining with the TACS Annexin V-Biotin Apoptosis Detection Kit (R&D Systems, Minneapolis, MN). Propidium iodide was used for nuclei staining, and Cy5 was conjugated to annexin V-biotin. Apoptosis of annexin V-positive cells was analyzed by flow cytometric analysis. Hoechst 33342 (Molecular Probes, Eugene, OR) was used for nuclear staining. DNA fragmentation assay was performed as described previously (11).

Androgen Protection Assay. LNCaP and PC3 cells were plated in a 6-well plate. Once the confluence reached 60–70%, GFP-tagged *U19* was transiently transfected into LNCaP and PC3 cells using LipofectAMINE 2000 (Invitrogen). After the cells were incubated with mixture containing 1 μg of DNA, 5 μl of LipofectAMINE, and 1 ml of OPTI-MEM medium (Invitrogen) for 4–5 h, the mixture was replaced by 3 ml of RPMI 1640 with 10% fetal bovine serum. At the same time, mibolerone was added to the medium at a final concentration of 1 nM, and the same amount of ethanol vehicle was added to the control. After 24 and 48 h of transfection, the cells were observed via fluorescence microscopy. The detached cells and/or cells with fragmented nuclei are considered dead.

Tumor Growth. To determine their tumorigenicity, parental or stably transfected AT6.1 cells were injected s.c. (1×10^5 cells) into 4–6-week-old male *nu/nu* mice. To induce GFP-*U19*-ER activity in nude mice, tamoxifen pellets (50 mg, 1 mg/per day release; Innovative Research) were s.c. implanted at the time of tumor cell injection. Tumor sizes were calculated using the formulas $V = \pi \times h\,(h^2 + 3a^2)/6$ and $a = (L + W)/4$ (12), and Student's t test (two-tailed) was performed to analyze statistical significance using SPSS 10.0 software (SPSS Inc., Chicago, IL).

Antibody Generation, Western Blot, and Immunohistochemistry. GST-*U19* fusion protein was generated by cloning human *U19* cDNA into pGEX-2T vector (Amersham-Pharmacia, Piscataway, NJ). Rabbit polyclonal antibodies were raised using the purified fusion protein (Spring Valley Laboratories, Woodbine, MD). The antibody was purified using GST-*U19* fusion protein covalently linked to a HiTrap column (Amersham-Pharmacia). The purified antibody was used for Western blot analysis as described previously (13) and for immunostaining of human radical prostatectomy specimens with a Vectastain ABC kit (Vector Laboratories, Burlingame, CA). The stained slides were briefly counterstained with hematoxylin.

LOH Analysis. Genomic DNA laser captured from matched normal and tumor prostate tissue was amplified by PCR and analyzed as described previously (14) using fluorescence-labeled primers for the indicated polymorphic microsatellite markers on chromosome 3q13 (NIH Genemap99). The exponential range of the PCR was determined for each marker and each sample and was between 30 and 40 cycles. The data were analyzed by the ABI Genescan and Genotype software packages (Perkin-Elmer, Boston, MA). A relative allele ratio of less than 0.7, which correlates with an allele loss of approximately 40%, was defined as LOH.

PCR Detection of Homozygous *U19* Deletion. With repeated attempts, we were unable to PCR amplify exon 2 and exon 3 using the microdissected tumor samples from patient 1 and patient 14, respectively. To confirm homozygous deletion of exon 2 in patient 1, a 50-μl mixture containing the primers for amplifying exon 2 and DNA sample from patient 1 was first PCR amplified at 94°C for 2 min for 1 cycle followed by 25 cycles of 94°C for 30 s, 55°C for 30 s, and 68°C for 30 s using Platinum High Fidelity Polymerase (Invitrogen). Then, 25 μl of the first PCR product were mixed with 25 μl of mixture containing the primers for β-actin and PCR amplified with 1 cycle of 94°C for 2 min; 35 cycles of 94°C for 30 s, 55°C for 30 s, and 68°C for 30 s; and a final extension of 68°C for 8 min. To confirm homozygous deletion of exon 3 in patient 14, two sets of PCR reactions were performed using genomic DNAs from patient 14. One PCR reaction was used to amplify exon 3, and another one was used for amplifying β-actin. The cycling conditions were as follows: 1 cycle of 94°C for 2 min; 35 cycles of 94°C for 30 s, 55°C for 30 s, and 68°C for 30 s; and a final extension at 68°C for 8 min. Based on the genomic sequence of human *U19*, a set of intronic primers near the intron/exon boundaries was designed to amplify exon 2 and exon 3 of the *U19* gene. For exon 2 amplification, the sense and antisense primers are 5′-TTTATCATTCTGAAACATGCTC-3′ and 5′-ACTTTAACCAATTATCACTACAC-3′, respectively. For exon 3 amplification, the sense and antisense primers are 5′-CAAGATTTCAAAGGCCTTCC-3′ and 5′-TTTTGCTTAGGATCTCCACC-3′. The primers for β-actin amplification were 5′-ATGGATGATGATATCGCCGCG-3′ and 5′-CACTCACCTGGGTCATCTTCTC-3′.

Analysis of *U19* Promoter Methylation. Microdissected tumors and matching normal prostate tissues were obtained from resected tissues. DNA was treated with sodium bisulfite following the protocol as described previously (15). Two pairs of primers were designed for amplifying the promoter region, which produced fragments of 335 bp (from –398 to –63 bp) and 211 bp (from –301 to –90 bp). Primers used for the first PCR were MT-*U19*-F2 (5′-TTAGGAGTTTGGGGTTTTGG-3′) and MT-*U19*-R4 (5′-AAACAACTAACTTAATCC-3′). Primers used for the second PCR were MT-*U19*-F4 (5′-TTTTATTAAAGAATTTGGGG-3′) and MT-*U19*-R5 (5′-AAATCACCCAAACTCCACC-3′).

RESULTS

Sequence, Expression, and Androgen Regulation of *U19*. We first cloned the full-length cDNA of rat *U19* and subsequently isolated the full-length cDNAs of mouse and human *U19* using low stringency hybridization coupled with 5′- and 3′-RACE. As shown in Fig. 1*A*, mouse and rat *U19* proteins are both 262 aa in length and share 91.6% identity. Human *U19* has a 3-aa deletion and a 1-aa insertion in the COOH-terminal region relative to the rodent *U19* proteins and shares 79.4% and 80.2% identity with rat and mouse *U19*, respectively. An interesting structural feature of *U19* is its serine-rich sequence from aa 174 through 205 (Fig. 1). The NH_2-terminal portion of *U19* (residues 1–113) is more conserved than its COOH-terminal region. The NH_2-terminal portion also shares significant homology (about 40% identity) with putative proteins identified in *Caenorhabditis elegans*, *Drosophila melanogaster*, and *Arabidopsis thaliana*. GenBank database search showed that human *U19* gene is localized to chromosome 3q13.

Human *U19* mRNA is expressed in virtually all surveyed tissues, with the most abundant expression in the prostate, kidney, bone marrow, and lymph nodes (Fig. 1*B*). In LNCaP human prostate cancer cells, androgens induce both *U19* mRNA and protein (Figs. 1, *C–E*), and the androgen induction of *U19* mRNA partially resisted inhibition of protein synthesis (Fig. 1*C*). These findings suggest that androgenic regulation of *U19* in the prostate is evolutionarily conserved and that *U19* is a primary androgen response gene. The androgen induction of *U19* expression occurs very rapidly, within 8 h after androgen treatment (Fig. 1*E*).

***U19* Is a Potent Apoptosis Inducer.** To further characterize the function of *U19*, we generated *U19* fusion proteins with GFP tagged at its NH_2 or COOH terminus. The GFP-*U19* or *U19*-GFP expression vectors were transiently transfected into human prostate cancer cell lines [LNCaP (16), PC3 (17), DU145 (18), and TSU (19)], rat Dunning prostate tumor cell lines [G, AT1, AT2, AT3.1, AT6.1, and MatLyLu (20)], and non-prostatic cell lines (NIH3T3 and HeLa). GFP-*U19* or *U19*-GFP was localized to the nuclei of all of the transfected cells (data not shown). All cells transfected with *U19*-GFP or GFP-*U19* expression vector exhibited chromatin condensation and plasma membrane blebbing (data not shown), indicative of apoptosis.

To determine whether *U19* alone, without GFP fusion, is capable of inducing apoptosis, we cloned *U19* into a bicistronic expression vector that drives the expression of GFP and *U19* as separate proteins in the same cell. As expected, the expression of untagged *U19* induced efficient apoptosis in the transfected cells (data not shown). These observations are consistent with our inability to stably transfect pros-

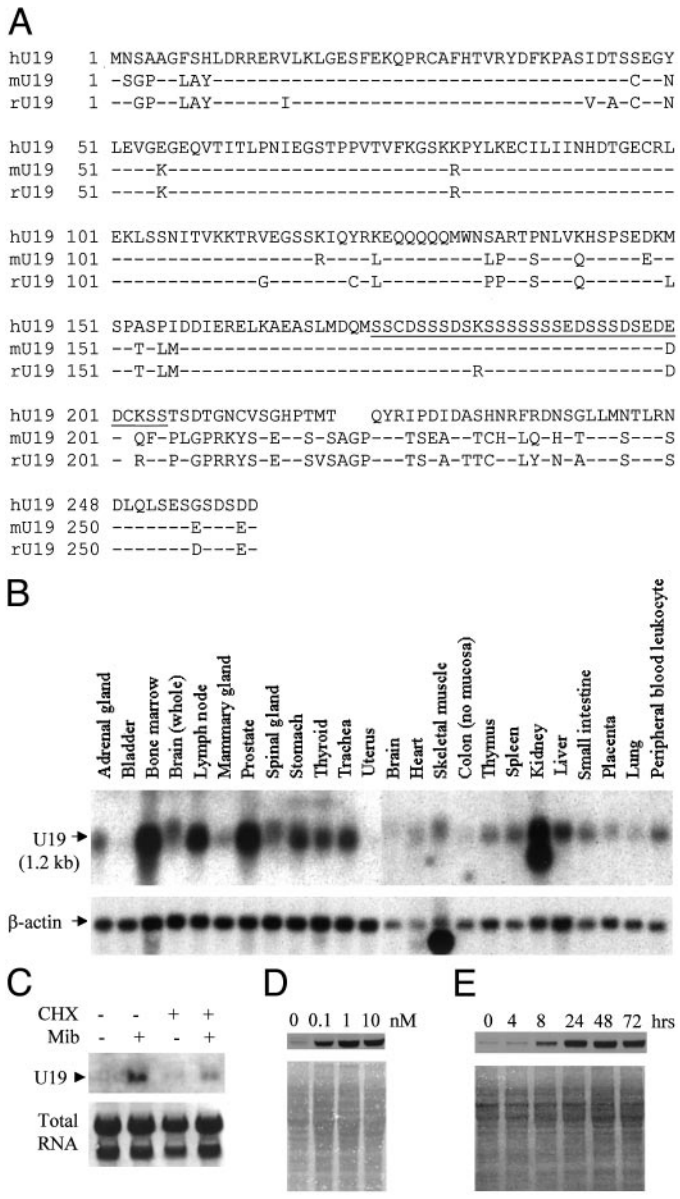

Fig. 1. The aa sequence, tissue specificity, and androgen responsiveness of *U19*. *A*, alignment of predicted human (*hU19*), mouse (*mU19*), and rat (*rU19*) *U19* aa sequences. Human *U19* has a 1-aa insertion at position 202 and a 3-aa deletion at position 221 relative to mouse *U19* and rat *U19*. Identical residues are indicated by −. GenBank accession numbers for human, mouse, and rat *U19* are AY049020, AY049021, and AY049022, respectively. The serine-rich region (aa 174–205) in h*U19* is *underlined*. *B*, Northern blot analysis of *U19* expression in multiple human tissues. Clontech human multiple tissue polyadenylated RNA Northern blots (catalogue no. 7780-1 and 7784-1) were hybridized with [α-^{32}P]dCTP-labeled human *U19* cDNA probe. The expression pattern of the β-actin gene was also included for normalization. *C*, Northern blot analysis of androgen induction of *U19* in LNCaP cells. LNCaP cells were treated with (+) or without (−) 10 nM of the androgen analogue mibolerone (*Mib*) for 18 h in the presence (+) or absence (−) of the protein synthesis inhibitor cycloheximide (*CHX*) at 10 μg/ml. *D*, Western blot analysis of dose response of androgen-induced *U19* expression in LNCaP cells. LNCaP cells were treated with the indicated dose of mibolerone for 72 h. *E*, Western blot analysis of the time course of androgen induction of *U19* expression in LNCaP cells. LNCaP cells were treated with 0.1 nM mibolerone for the indicated time periods. Ponceau S staining was used to indicate protein loading.

tate cancer cells with constitutive untagged or FLAG-tagged *U19* expression vector (data not shown).

To regulate *U19* activity for further functional studies, we established a tripartite fusion protein GFP-*U19*-ER consisting of GFP at the NH_2 terminus, *U19* in the middle, and a modified estrogen receptor ligand-binding domain (ER) at the COOH terminus. The activity of transcription factor-ER fusion proteins can be regulated by tamoxifen or 4-OHT but not endogenous estrogens (21, 22). In stably transfected PC3 cells, Western blot analysis showed that the GFP-*U19*-ER fusion protein is expressed (Fig. 2*e*). The GFP-*U19*-ER was primarily localized to the cytoplasm in the absence of ligand 4-OHT and was translocated into nuclei in the presence of 4-OHT (Fig. 2*a*). The activation of GFP-*U19*-ER caused chromatin condensation and enhancement of Hoechst staining of the nuclei (Fig. 2*a*). The *U19*-induced apoptosis is sensitive to caspase inhibitor Z-VAD (Fig. 2, *a* and *b*), indicating the involvement of caspases in *U19* induced apoptosis. Agarose gel electrophoresis revealed genomic DNA fragmentation in *U19*-induced cell death (Fig. 2*d*). The above-mentioned results demonstrate that *U19* induces extensive cell death via caspase-dependent apoptosis.

The GFP-*U19*-ER inducible system appears to be leaky because a significant percentage (12.0%) of the cells in PC3 sublines stably expressing GFP-*U19*-ER were apoptotic in the absence of ligand (Fig. 2, *a* and *b*). In contrast, less than 1% apoptotic cells were detected by Hoechst staining in PC3 sublines stably expressing GFP-ER (Fig. 2*b*) or in parental PC3 cells (data not shown). This leaky *U19* activity most likely reflects a low level of ligand-independent nuclear translocation of GFP-*U19*-ER (Fig. 2*a*). As expected, the leaky activity-induced apoptosis can be blocked by caspase inhibitor Z-VAD (Fig. 2, *a* and *b*). The induction of apoptosis by leaky *U19* activity in transfected cells argues that *U19* is a highly potent apoptosis inducer.

U19-induced apoptosis is sensitive to protein synthesis inhibition. In the absence of protein synthesis inhibitor cycloheximide, flow cytometric analysis by Annexin V staining detected 13.2% apoptotic cells in the absence of 4-OHT and 69.6% apoptotic cells in the presence of 4-OHT (Fig. 2*c*). In the presence of cycloheximide, the percentage of apoptotic cells was 19.1% in the absence of 4-OHT and 25.1% in the presence of 4-OHT, indicating that cycloheximide inhibited the apoptosis induced by 4-OHT. This observation suggests that *U19*-dependent transcription and new protein synthesis are required for the apoptosis induction.

Androgen Inhibits *U19*-induced Apoptosis in LNCaP Cells. Although *U19* induced dramatic apoptosis in prostate cancer cells, its androgen-dependent expression does not cause apoptosis in the normal prostate. Also, the induction of *U19* in androgen-sensitive human LNCaP cells by androgens does not induce cell death. This led us to hypothesize that androgens are protective against *U19*-induced apoptosis. We showed in Fig. 3 that mibolerone, a synthetic androgen, significantly inhibited *U19*-induced apoptosis in LNCaP cells. After 48 h of transfection, only 10.1% of the *U19*-transfected cells were dead in the presence of 1 nM mibolerone, whereas about 80.1% of the *U19*-transfected cell were dead in the absence of mibolerone. In contrast, mibolerone did not affect the apoptosis induced by *U19* in androgen-insensitive PC3 cells, indicating that the androgen protection requires the androgen receptor. This observation provides an explanation for the fact that androgen induction of *U19* in LNCaP cells does not induce cell death.

Suppression of Xenograft Tumor Growth by *U19* Expression. The availability of prostate cancer cells stably expressing GFP-*U19*-ER provided an opportunity to test whether *U19* can suppress tumor growth. The parental PC3 prostate cancer cells are aggressive and readily generate xenograft tumors when implanted s.c (23). As expected, implantation of the parental PC3 cells or PC3 sublines expressing GFP-ER yielded aggressive xenograft tumors in all injected nude mice (data not shown). However, the PC3 sublines expressing GFP-*U19*-ER were unable to generate xenograft tumors after s.c. injection into nude mice, suggesting that the leaky activity of GFP-*U19*-ER suppressed PC3 tumor growth *in vivo* in the absence of ligand. Thus, we examined the impact of *U19* in the more aggressive AT6.1 rat Dunning prostate tumor cell line (12, 20). The AT6.1 sublines expressing GFP-*U19*-ER were able to generate

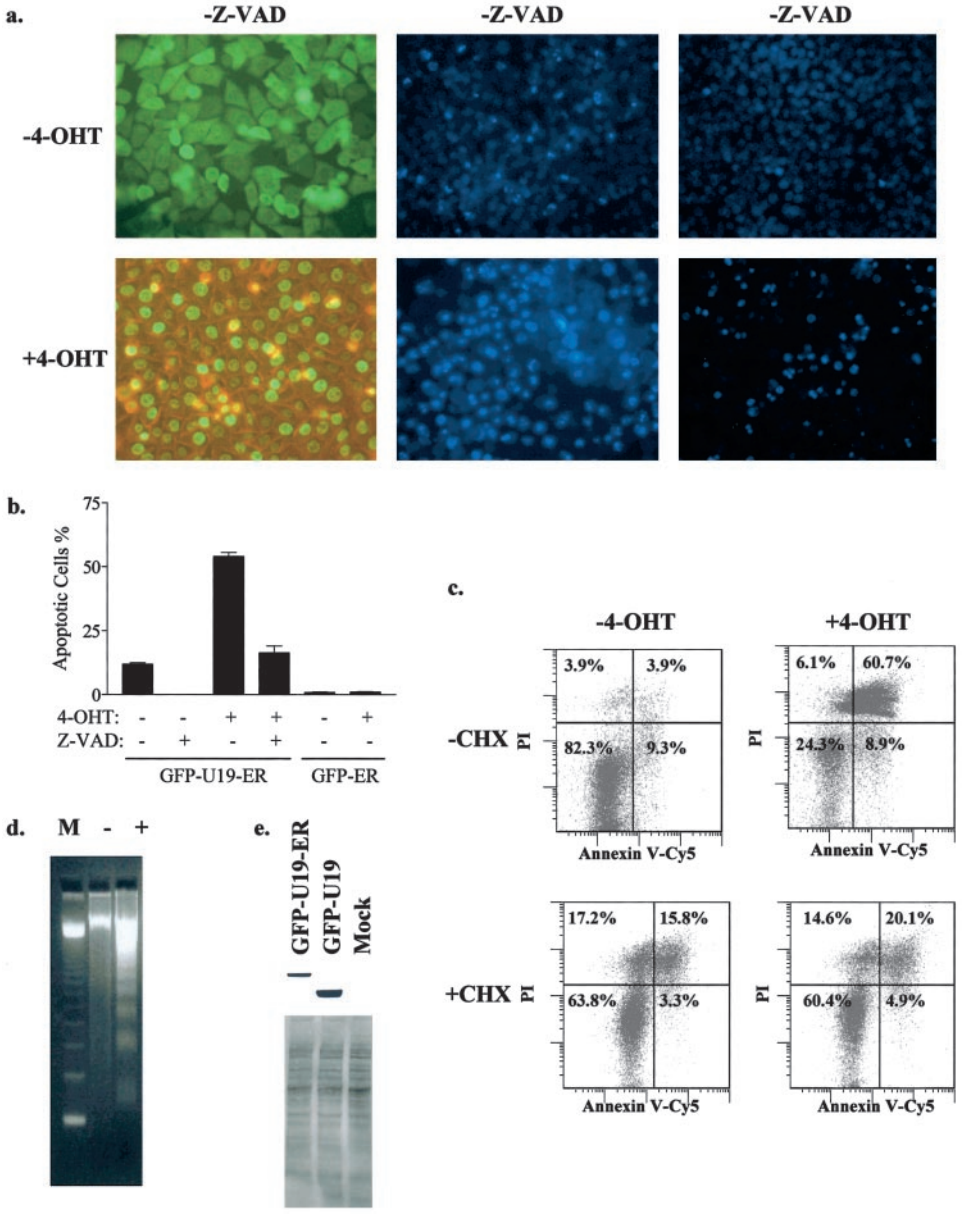

Fig. 2. Apoptosis induction by *U19*. *a*, activation of the tripartite GFP-*U19*-ER fusion protein by 4-OHT in stably transfected PC3 cells. The *top left panel* shows the localization of GFP-*U19*-ER protein in the absence of 4-OHT, as visualized under green fluorescent microscope. The *bottom left panel* shows the localization of the fusion protein 24 h after treatment with 300 nM 4-OHT. The *top middle panel* shows Hoechst staining in the absence of 4-OHT. The *bottom middle panel* shows Hoechst staining 72 h after 4-OHT treatment. The *top right panel* shows the effect of caspase inhibitor Z-VAD (100 μM) in the absence of 4-OHT, and the *bottom right panel* shows the effect of caspase inhibitor Z-VAD (100 μM) in the presence of 4-OHT. Z-VAD was added 1 h before the addition of 4-OHT. *b*, quantification of apoptosis in PC3 cells with stable expression of GFP-*U19*-ER or GFP-ER cultured under the indicated conditions. The percentage of apoptotic cells reflects the percentage of Hoechst-positive cells. *c*, flow cytometric analysis of annexin V staining for PC3 cells transfected with the tripartite fusion protein. As indicated, the PC3 cells were cultured in the absence or presence of 300 nM 4-OHT for 72 h before flow cytometric analysis. The experiment was also carried out in the presence of 5 μg/ml cycloheximide (*CHX*), which was added 1 h before the addition of 4-OHT. The results are representative of three separate experiments. *d*, DNA fragmentation assay. A PC3 subline transfected with GFP-*U19*-ER fusion protein was cultured in the absence (−) or presence (+) of 300 nM 4-OHT for 48 h. Genomic DNA of the cultured cells was prepared and separated on an agarose gel (11). *M* indicates the 123-bp DNA marker (Invitrogen). *e*, Western blot analysis of GFP-*U19*-ER fusion protein in stably transfected PC3 cells. PC3 cells transiently transfected with GFP-*U19* or empty (*Mock*) vector for 24 h were included as controls. Ponceau S staining (*bottom panel*) was used to indicate protein loading.

xenograft tumors in the absence of tamoxifen, but at a much slower rate relative to the parental or GFP-ER-transfected AT6.1 cells (Fig. 4*a*), suggesting that the AT6.1 xenograft tumors were also inhibited by leaky *U19* activity. As expected, the growth of xenograft tumors derived from an AT6.1 subline expressing GFP-*U19*-ER was significantly inhibited ($P < 0.005$) by tamoxifen administration that would activate the *U19* fusion protein (Fig. 4*b*). In contrast, tamoxifen administration had no detectable influence on the growth of xenograft tumors derived from the GFP-ER-transfected AT6.1 cells in parallel experiments (Fig. 4*a*). These observations showed that *U19* markedly suppressed AT6.1 xenograft prostate tumor growth *in vivo*.

TUNEL assay was used to determine whether *U19* induces apoptosis *in vivo*. In xenograft tumors of AT6.1 cells expressing GFP-*U19*-ER, 34.9% of the cells were TUNEL positive in the absence of ligand (Fig. 4*c*), suggesting that the leaky GFP-*U19*-ER activity also induced apoptosis *in vivo*. This observation is consistent with dramatically reduced growth of GFP-*U19*-ER xenograft tumors in the absence of tamoxifen. As expected, tamoxifen administration enhanced the TUNEL-positive cells to 61.0% *in vivo* (Fig. 4*c*). The control experiments showed no TUNEL staining in xenografts derived from AT6.1 cells expressing GFP-ER in either the absence or presence of tamoxifen (Fig. 4*c*; data not shown). These observations indicate that *U19* induces apoptosis in prostate cancer cells *in vivo*.

Down-Regulation, LOH, Deletion, and Promoter Methylation of *U19* in Human Prostate Cancer Specimens. If *U19* is indeed playing an important tumor-suppressive role in prostate cancer, its expression should be frequently down-regulated in prostate cancer cells. Northern blot analysis showed that *U19* expression in human prostate cancer cell lines LNCaP, PC3, DU145, and TSU is down-regulated relative to its expression in human benign prostatic hyperplasia tissues (Fig. 5*a*). Consistent with the suppressive role of *U19* in prostate cancer progression, the level of *U19* mRNA in LNCaP is greater than that in PC3, DU145, and TSU, which inversely correlates with the aggressiveness of these cell lines (Fig. 5*a*). *U19* expression is also down-regulated in the Dunning rat prostate cancer cell lines (Fig. 5*b*). Down-regulation of *U19* in all of the surveyed prostate cancer cell lines suggests that it is a key molecule in the growth control of prostate cancer.

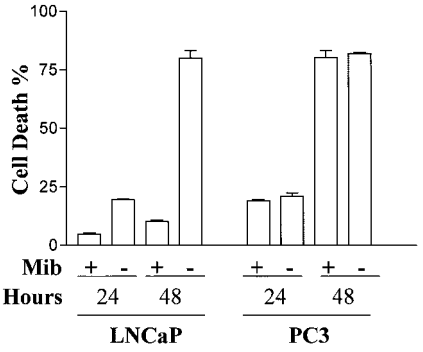

Fig. 3. Effect of androgen on *U19*-induced apoptosis in LNCaP and PC3 cells. Mibolerone was added to the medium at a final concentration 1 nM (+), and the same amount of ethanol vehicle was added to the control (−). After 24 and 48 h of transfection, the cells were observed via fluorescence microscopy as described in "Materials and Methods."

To determine whether *U19* protein is down-regulated in human prostate cancer specimens, we have generated an antihuman *U19* antibody for immunohistochemistry studies. Typical *U19* down-regulation is shown in Fig. 6*e*. Benign prostatic epithelial cells were strongly stained in the presence of anti-*U19* antibody. In contrast, prostatic cancer cells exhibited weak or no staining by anti-*U19* antibody. Significant *U19* down-regulation in advanced prostate cancer cells (Fig. 6*d*) was observed in 19 of 23 radical prostatectomy specimens with Gleason scores of 7–10 (Fig. 6*c*) obtained from patients naïve to androgen ablation.

To investigate whether *U19* locus exhibits allelic loss, deletion, or mutation in neoplastic foci of clinical prostate cancer specimens, we performed LCM on samples from the same 23 patients. A very high rate of allelic loss was found for polymorphic markers encompassing the *U19* locus on chromosome 3q13 (Fig. 6, *a* and *b*). Of the 23 samples analyzed, 19 (82.6%) displayed LOH of the *U19* locus (Fig. 6*b*). Furthermore, two of these 23 specimens had homozygous deletion of the *U19* gene, one at exon 2 and the other at exon 3 (Fig. 6*f*).

Gene silencing that arises from methylation is an important epigenetic mechanism of tumor suppressor inactivation. Epigenetic inactivation of gene expression often involves complete transcription silencing by methylation of CpG islands in promoter regions. According to our computer analysis, the *U19* promoter region from –302 to –110 bp relative to the transcription start site contains a CpG island with a CpG frequency more than 100 times higher than that of other *U19* genomic regions. The bisulfite sequencing method was used to detect *U19* promoter methylation using DNA from the 23 paired LCM samples. Due to technical difficulties, only 8 of 23 paired samples could be amplified by PCR. One of the specimens showed clear *U19* promoter methylation in the tumor cells but not benign cells (Fig. 6*g*).

DISCUSSION

The present study describes the characterization of *U19*, an androgen response gene in the prostate. Our studies showed that *U19* overexpression induces massive apoptosis and inhibits prostate tumor growth *in vivo*. We have also presented evidence for frequent *U19* down-regulation and allelic loss in human prostate cancer specimens. Furthermore, we detected homozygous *U19* deletion and promoter hypermethylation. These observations argue that part of the androgen action pathway is proapoptotic and/or growth suppressive and is frequently inactivated in prostate cancer progression.

***U19* Induces Apoptosis and Inhibits Prostate Tumor Growth.** Our transient transfection studies showed that *U19* induced apoptosis in all of the surveyed prostatic and non-prostatic cell lines. This observation is consistent with our inability to establish stable prostate cancer cell clones with constitutive *U19* expression vectors. However, we were able to establish prostate cancer cell lines with stable expression of the GFP-*U19*-ER fusion protein that allows the regulation of U19 activity by tamoxifen or 4-OHT. The GFP-*U19*-ER fusion protein has leaky *U19* activity that induces apoptosis and can be further activated by 4-OHT to induce more dramatic apoptosis in prostate cancer cells in both culture dish and xenograft tumors. The fact that leaky *U19* activity is sufficient to induce apoptosis argues that *U19* is a highly potent apoptosis inducer. Consistent with its proapoptotic activity, *U19* overexpression dramatically inhibited xenograft tumor growth of both PC3 and AT6.1 prostate cancer cells.

U19-induced apoptosis is a caspase-dependent process because of its sensitivity to the caspase inhibitor Z-VAD (Fig. 2, *a* and *b*). The mechanism by which *U19* activates the caspase cascade remains to be elucidated. However, transcriptional activation of new genes appears

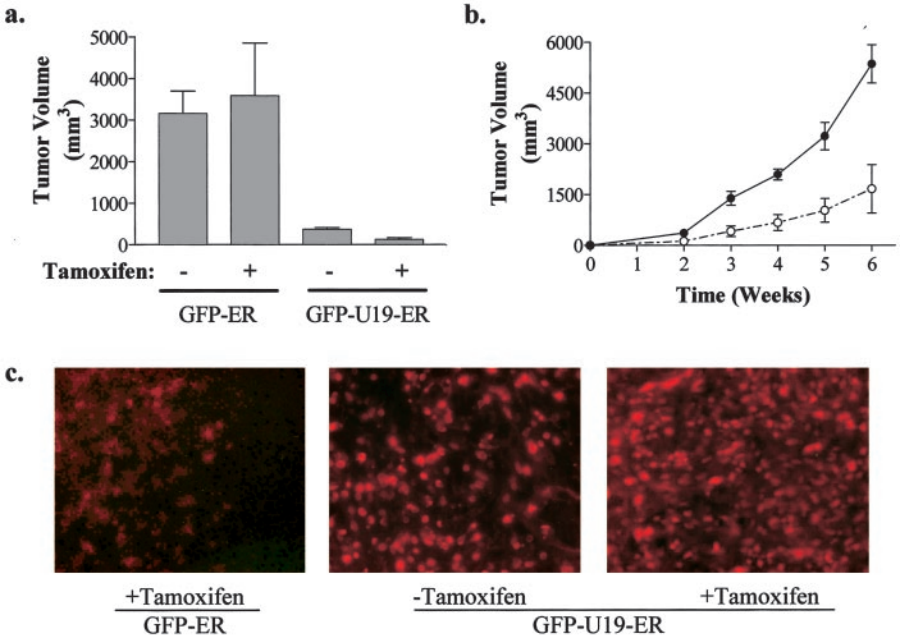

Fig. 4. *U19* as a tumor suppressor in the prostate. *a*, inhibition of AT6.1 prostatic xenograft tumor growth by GFP-*U19*-ER expression. GFP-ER or GFP-*U19*-ER stably transfected AT6.1 cells were inoculated s.c. into nude mice in the presence (+) or absence (−) of tamoxifen pellets implanted at the time of tumor cell injection. The *error bars* represent SE. Because AT6.1 cells are highly aggressive, the tumor sizes were determined 2 weeks after the inoculation. *b*, inhibition of AT6.1 prostatic xenograft tumor growth by tamoxifen activation of GFP-*U19*-ER in nude mice. s.c. injected AT6.1 cells stably transfected with GFP-*U19*-ER were allowed to grow in nude mice in the presence (*dotted line with open circles*) or absence (*solid line and filled circles*) of tamoxifen. The inhibition of AT6.1 tumor growth by tamoxifen induction of *U19* fusion protein was statistically significant ($P < 0.005$) at every time point of tumor measurement. *c*, TUNEL analysis of xenograft tumors. TUNEL was performed using the *In Situ* Cell Death Detection Kit, TMR red (Boehringer Mannheim). The tumors were grown under the indicated conditions.

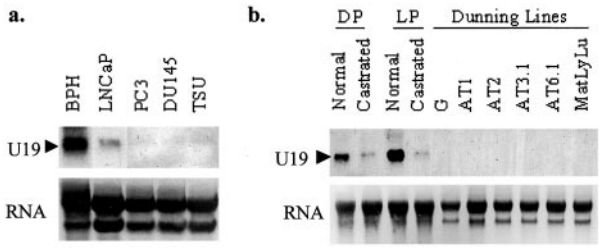

Fig. 5. Down-regulation of *U19* expression in prostate cancer cell lines. *a,* Northern blot analysis of *U19* expression in human benign prostatic hyperplasia and prostate cancer cell lines. *b,* Northern blot analysis of *U19* expression in rat dorsal (*DP*) and lateral (*LP*) prostatic tissues and the rat Dunning cancer cell lines. The loading and quality of total RNA were visualized by methylene blue staining.

to be required for the apoptosis because *U19* induction of apoptosis can be blocked by a protein synthesis inhibitor (Fig. 2*c*). Identification of *U19* partners and/or downstream genes would provide insights into the mechanism of *U19* action.

Roles of *U19* in Androgen Action. It is difficult to predict whether endogenous *U19* plays a role in apoptosis in the prostate, although its overexpression is highly apoptotic in cultured prostate cancer cells and in xenograft tumors. *U19* is unlikely to be involved in the castration-induced apoptosis in the normal prostate because *U19* expression is down-regulated by castration. Although *U19* is expressed in the normal prostatic epithelial cells, these cells do not undergo extensive apoptosis in testis-intact animals. One possibility is that *U19* may function differently in the normal prostate relative to prostate cancer. Alternatively, androgens can protect prostatic epithelial cells from *U19*-induced apoptosis. Kimura *et al.* (24) recently reported that androgens can inhibit apoptosis of androgen-sensitive LNCaP human prostate cancer cells via blockage of caspase activation in both intrinsic and extrinsic cell death pathways. As expected, *U19*-induced apoptosis, a caspase-dependent process (Fig. 2), is markedly inhibited by androgen in LNCaP cells (Fig. 3).

U19 is likely to play a growth-suppressive role in androgen action in the prostate because it is an apoptosis inducer that markedly suppresses xenograft tumor growth. Androgens are well known to regulate the growth of the prostate. However, the effect of androgens on prostate growth is complex. Androgens are growth-stimulating only in a regressed prostate, but not in a fully grown prostate, suggesting that androgens induce nullifiers that restrict growth once the prostate reaches the normal size (8). Because *U19* is proapoptotic and/or growth suppressive, it may function as a nullifier that contributes to the androgen-dependent growth restriction in the prostate. Future studies such as targeted deletion of the *U19* gene in mice will further define the roles of *U19* in androgen action in the prostate.

Roles of *U19* in Prostate Cancer Progression. Our studies suggest that *U19* is a potential tumor suppressor in the prostate. Consistent with its potent apoptotic and tumor-suppressive activities, the expression of *U19* appears to be incompatible with prostate cancer cells. No *U19* mRNA expression was detected by Northern blot in the Dunning rat prostatic cancer cell lines, and *U19* expression in the human prostate cancer cell lines is much lower than that in the benign prostatic tissues. *U19* down-regulation and allelic loss were observed in >80% human prostate cancer specimens, which is similar or higher than the inactivation of known tumor suppressors including *RB* (25–27), *p53* (28–30), *PTEN* (31), and *NKX3.1* (32). Our data suggest that *U19* is a strong candidate tumor suppressor in the 3q13 region.

The effect of abnormal *U19* inactivation by genetic or epigentic mechanisms in prostate cancer cells is different from the effect of *U19* down-regulation caused by falling levels of androgens. Androgens induce not only growth-inhibitory proteins such as *U19* but also

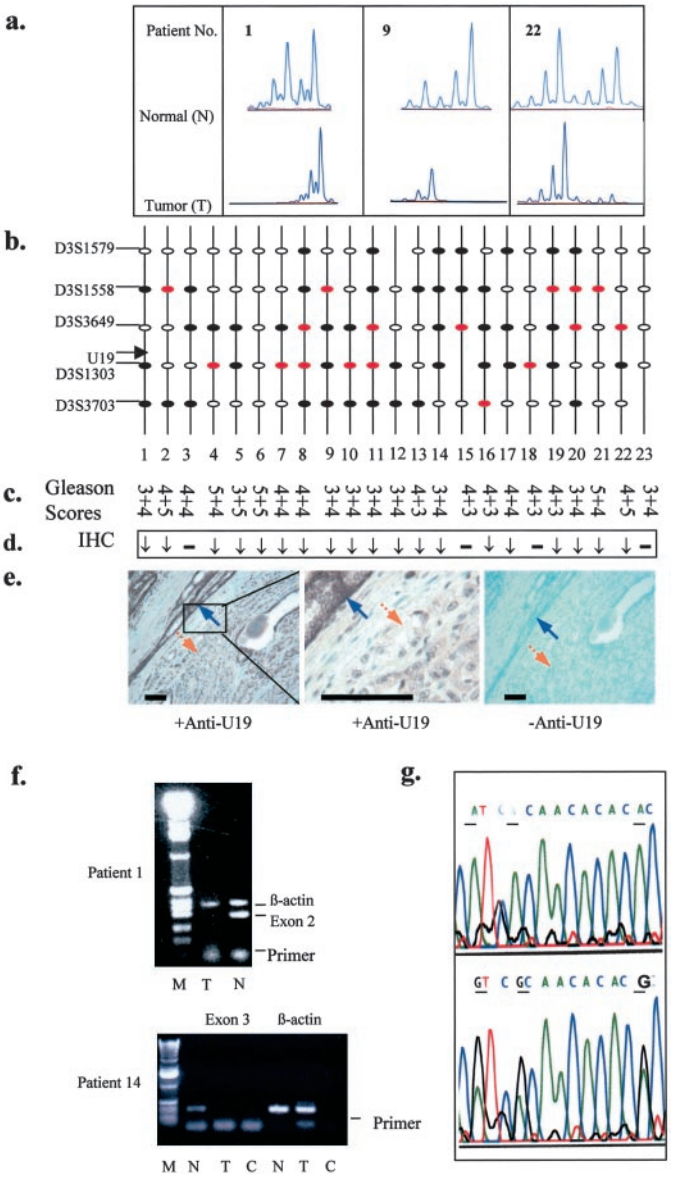

Fig. 6. *U19* allelic loss, down-regulation, homozygous deletion, and promoter methylation in human prostate tumors. *a,* representative fluorescent electropherograms for microsatellite makers D3S3703 and D3S1303 for patients with LOH. The normal (*top*) and tumor (*bottom*) counterparts of patients 1, 9, and 22 are indicated. All of the samples were isolated by LCM. *b,* summary of LOH patterns of 23 prostate tumors. Retained microsatellite markers are indicated in *white,* markers demonstrating allelic loss are indicated in *black,* and noninformative (homozygous) markers are indicated in *red.* The position without cycle indicates DNA that could not be amplified. Genomic map was not drawn to scale. *c,* Gleason scores of 23 prostate cancer samples. *d,* summary of *U19* expression in prostate cancer. The expression of *U19* was determined by immunohistochemistry. The down-regulation (↓) and no change (−) in *U19* expression in the radical prostatectomy specimens from 23 patients with advanced prostate cancer are indicated. *e,* immunostaining of *U19* in prostate cancer specimen. A typical *U19* down-regulation was shown with ×200 magnification (*left panel*), and the *boxed area* is shown at high magnification (*middle panel*). Affinity-purified antihuman *U19* polyclonal antibody was used in immunostaining. A parallel staining without primary antibody (*right panel*) was conducted as a control. The *bars* at *bottom left* denote 100 μm. *Blue arrows with solid line* point to benign epithelial cells, whereas *red arrows with dotted line* indicate cancerous cells. *f, U19* homozygous deletion in prostate cancer specimens. The *top gel* shows that in the same reaction, β-actin was easily amplified in the matched normal and tumor samples of patient 1, but exon 2 was amplified in the normal sample only. The *bottom gel* shows that β-actin was easily amplified in the normal and tumor samples of patient 14, but exon 3 was amplified in the normal sample only. *g,* methylation of *U19* promoter in prostate cancer. Bisulfite sequencing analysis was carried out on a DNA fragment consisting of −242 to −225 bp relative to the *U19* transcription start site using the MT-*U19*-R5 primer (see "Materials and Methods"). The *top panel* shows that the DNA fragment exhibited C→T conversions (*underlined*) in the normal prostate cells of patient 12. The *bottom panel* shows that the DNA fragment was not converted (*underlined*) in the matched prostate cancer cells.

growth-stimulatory proteins. Down-regulation of growth-inhibitory genes along with down-regulation of growth-stimulatory genes due to low androgen levels is unlikely to predispose someone to prostate cancer. However, abnormal down-regulation of growth-inhibitory genes, without coordinated down-regulation of growth-stimulatory genes, could lead to uncontrolled growth in the prostate.

Our finding that *U19* expression is frequently down-regulated in prostate cancer specimens and cell lines suggests that inactivation of androgen-dependent growth restriction pathway, via *U19* down-regulation, is common in prostate cancer progression. Androgen receptor is present and functional in most human prostate tumors before androgen ablation therapy because the tumor cells express androgen-dependent prostate-specific antigen. Thus, the down-regulation of *U19* is unlikely to be due to the lack of functional androgen receptor because most, if not all, radical prostatectomy tumor specimens were derived from patients positive for serum prostate-specific antigen and naïve to androgen ablation treatment. In the absence of *U19* but in the presence of androgen receptor, androgens are likely to cause excessive proliferation in the prostate and enhance cancer progression.

During the preparation of this manuscript, Simone *et al.* (33) reported that human *EAF1*, a homologue of *U19*, is a novel *ELL*-associated factor. Very recently, the same group reported human *EAF2*, which is identical to human *U19* (34). *EAF1* and *U19*/*EAF2* share 58% identity and 74% aa conservation. As indicated in Fig. 1, *U19* consists of a stretch of a serine-rich region spanning aa residues 174 through 205. However, no recognizable motif was identified in *EAF1* and *U19*/*EAF2*. The NH_2-terminal region (aa 17–104) of *U19*/*EAF2* can interact with ELL, and it remains to be determined whether *ELL-EAF2*/*U19* interaction is critically important in apoptosis induction by *U19*. The COOH terminus (aa 177–260) of *U19*/*EAF2* contains a transactivation domain (33, 34), suggesting that *U19*/*EAF2* may function by influencing transcription. This concept is consistent with our data that new protein synthesis is required for *U19* induction of apoptosis (Fig. 2*c*). More structural/functional studies will be required to characterize *U19*/*EAF2*.

ACKNOWLEDGMENTS

We are grateful to G. Evan for providing a plasmid containing the ER domain. We thank X. Cai, J. Cyriac, and R. Haleem for technical assistance; Mary Paniagua for flow cytometry assay; and Andrew Andres, Kathleen Green, David Klumpp, Kathy Rundell, Olga Volpert, and members of Wang laboratory for comments on the manuscript.

REFERENCES

1. Ross, R. K., Pike, M. C., Coetzee, G. A., Reichardt, J. K., Yu, M. C., Feigelson, H., Stanczyk, F. Z., Kolonel, L. N., and Henderson, B. E. Androgen metabolism and prostate cancer: establishing a model of genetic susceptibility. Cancer Res., *58:* 4497–4504, 1998.
2. Pollard, M. Lobund-Wistar rat model of prostate cancer in man. Prostate, *37:* 1–4, 1998.
3. Noble, R. L. The development of prostatic adenocarcinoma in Nb rats following prolonged sex hormone administration. Cancer Res., *37:* 1929–1933, 1977.
4. Dai, W. S., Kuller, L. H., LaPorte, R. E., Gutai, J. P., Falvo-Gerard, L., and Caggiula, A. The epidemiology of plasma testosterone levels in middle-aged men. Am. J. Epidemiol., *114:* 804–816, 1981.
5. Sternbach, H. Age-associated testosterone decline in men: clinical issues for psychiatry. Am. J. Psychiatry, *155:* 1310–1318, 1998.
6. Morley, J. E., Kaiser, F. E., Perry, H. M., III, Patrick, P., Morley, P. M., Stauber, P. M., Vellas, B., Baumgartner, R. N., and Garry, P. J. Longitudinal changes in testosterone, luteinizing hormone, and follicle-stimulating hormone in healthy older men. Metabolism, *46:* 410–413, 1997.
7. English, H. F., Kyprianou, N., and Isaacs, J. T. Relationship between DNA fragmentation and apoptosis in the programmed cell death in the rat prostate following castration. Prostate, *15:* 233–250, 1989.
8. Bruchovsky, N., Lesser, B., Doorn, E. V., and Craven, S. Hormonal effects on cell proliferation in rat prostate. Vitam. Horm., *33:* 61–102, 1975.
9. Zhou, Z., Wong, C., Sar, M., and Wilson, E. The androgen receptor: an overview. Recent Prog. Horm. Res., *49:* 249–274, 1994.
10. Wang, Z., Tufts, R., Haleem, R., and Cai, X. Genes regulated by androgen in the rat ventral prostate. Proc. Natl. Acad. Sci. USA, *94:* 12999–13004, 1997.
11. Zhu, N., and Wang, Z. An assay for DNA fragmentation in apoptosis without phenol/chloroform extraction and ethanol precipitation. Anal. Biochem., *246:* 155–158, 1997.
12. Taguchi, A., Blood, D. C., del Toro, G., Canet, A., Lee, D. C., Qu, W., Tanji, N., Lu, Y., Lalla, E., Fu, C., Hofmann, M. A., Kislinger, T., Ingram, M., Lu, A., Tanaka, H., Hori, O., Ogawa, S., Stern, D. M., and Schmidt, A. M. Blockade of RAGE-amphoterin signalling suppresses tumour growth and metastases. Nature (Lond.), *405:* 354–360, 2000.
13. Zhu, N., and Wang, Z. Calreticulin expression is associated with androgen regulation of the sensitivity to calcium ionophore-induced apoptosis in LNCaP prostate cancer cells. Cancer Res., *59:* 1896–1902, 1999.
14. Narla, G., Heath, K. E., Reeves, H. L., Li, D., Giono, L. E., Kimmelman, A. C., Glucksman, M. J., Narla, J., Eng, F. J., Chan, A. M., Ferrari, A. C., Martignetti, J. A., and Friedman, S. L. KLF6, a candidate tumor suppressor gene mutated in prostate cancer. Science (Wash. DC), *294:* 2563–2566, 2001.
15. Herman, J. G., Graff, J. R., Myohanen, S., Nelkin, B. D., and Baylin, S. B. Methylation-specific PCR: a novel PCR assay for methylation status of CpG islands. Proc. Natl. Acad. Sci. USA, *93:* 9821–9826, 1996.
16. Horoszewicz, J. S., Leong, S. S., Kawinski, E., Karr, J. P., Rosenthal, H., Chu, T. M., Mirand, E. A., and Murphy, G. P. LNCaP model of human prostatic carcinoma. Cancer Res., *43:* 1809–1818, 1983.
17. Kaighn, M. E., Narayan, K. S., Ohnuki, Y., Lechner, J. F., and Jones, L. W. Establishment and characterization of a human prostatic carcinoma cell line (PC-3). Investig. Urol., *17:* 16–23, 1979.
18. Stone, K. R., Mickey, D. D., Wunderli, H., Mickey, G. H., and Paulson, D. F. Isolation of a human prostate carcinoma cell line (DU 145). Int. J. Cancer, *21:* 274–281, 1978.
19. Iizumi, T., Yazaki, T., Kanoh, S., Kondo, I., and Koiso, K. Establishment of a new prostatic carcinoma cell line (TSU-Pr1). J. Urol., *137:* 1304–1306, 1987.
20. Isaacs, J. T., Isaacs, W. B., Feitz, W. F., and Scheres, J. Establishment and characterization of seven Dunning rat prostatic cancer cell lines and their use in developing methods for predicting metastatic abilities of prostatic cancers. Prostate, *9:* 261–281, 1986.
21. Littlewood, T. D., Hancock, D. C., Danielian, P. S., Parker, M. G., and Evan, G. I. A modified oestrogen receptor ligand-binding domain as an improved switch for the regulation of heterologous proteins. Nucleic Acids Res., *23:* 1686–1690, 1995.
22. Sengupta, S., Ralhan, R., and Wasylyk, B. Tumour regression in a ligand inducible manner mediated by a chimeric tumour suppressor derived from p53. Oncogene, *19:* 337–350, 2000.
23. Shevrin, D. H., Gorny, K. I., and Kukreja, S. C. Patterns of metastasis by the human prostate cancer cell line PC-3 in athymic nude mice. Prostate, *15:* 187–194, 1989.
24. Kimura, K., Markowski, M., Bowen, C., and Gelmann, E. P. Androgen blocks apoptosis of hormone-dependent prostate cancer cells. Cancer Res., *61:* 5611–5618, 2001.
25. Hugel, A., and Wernert, N. Loss of heterozygosity (LOH), malignancy grade and clonality in microdissected prostate cancer. Br. J. Cancer, *79:* 551–557, 1999.
26. Ittmann, M. M., and Wieczorek, R. Alterations of the retinoblastoma gene in clinically localized, stage B prostate adenocarcinomas. Hum. Pathol., *27:* 28–34, 1996.
27. Bookstein, R., Rio, P., Madreperla, S. A., Hong, F., Allred, C., Grizzle, W. E., and Lee, W. H. Promoter deletion and loss of retinoblastoma gene expression in human prostate carcinoma. Proc. Natl. Acad. Sci. USA, *87:* 7762–7766, 1990.
28. Brooks, J. D., Bova, G. S., Ewing, C. M., Piantadosi, S., Carter, B. S., Robinson, J. C., Epstein, J. I., and Isaacs, W. B. An uncertain role for *p53* gene alterations in human prostate cancers. Cancer Res., *56:* 3814–3822, 1996.
29. Macera, M. J., Godec, C. J., Sharma, N., and Verma, R. S. Loss of heterozygosity of the TP53 tumor suppressor gene and detection of point mutations by the non-isotopic RNAse cleavage assay in prostate cancer. Cancer Genet. Cytogenet., *108:* 42–47, 1999.
30. Massenkeil, G., Oberhuber, H., Hailemariam, S., Sulser, T., Diener, P. A., Bannwart, F., Schafer, R., and Schwarte-Waldhoff, I. P53 mutations and loss of heterozygosity on chromosomes 8p, 16q, 17p, and 18q are confined to advanced prostate cancer. Anticancer Res., *14:* 2785–2790, 1994.
31. Leube, B., Drechsler, M., Muhlmann, K., Schafer, R., Schulz, W. A., Santourlidis, S., Anastasiadis, A., Ackermann, R., Visakorpi, T., Muller, W., and Royer-Pokora, B. Refined mapping of allele loss at chromosome 10q23–26 in prostate cancer. Prostate, *50:* 135–144, 2002.
32. Abate-Shen, C., and Shen, M. M. Molecular genetics of prostate cancer. Genes Dev., *14:* 2410–2434, 2000.
33. Simone, F., Polak, P. E., Kaberlein, J. J., Luo, R. T., Levitan, D. A., and Thirman, M. J. EAF1, a novel ELL-associated factor that is delocalized by expression of the MLL-ELL fusion protein. Blood, *98:* 201–209, 2001.
34. Simone, F., Luo, R. T., Polak, P. E., Kaberlein, J. J., and Thirman, M. J. ELL-associated factor 2 (EAF2), a functional homologue of EAF1 with alternative ELL binding properties. Blood, *101:* 2355–2362, 2003.